DECOMPOSITION OF A UWB PULSE IN STRUCTURES WITH FACIAL FEEDBACK

A. T. Gazizov, A. M. Zabolotsky, and T. R. Gazizov   UDC 621.372.2

The urgency of protection of radio-electronic equipment from UWB pulses is indicated. The principle of modal filtration based on the application of the physical phenomenon of signal decomposition in transmission lines is shortly described. An asymmetric modal filter with facial feedback is analyzed. Its models with different parameters have been developed and manufactured. A field experiment and a computer simulation of the time response to a 1 ns pulse width have been performed. The agreement between the experimental and simulation results is demonstrated. For a modal filter with optimal parameters, the input pulse attenuation by 5 times is demonstrated in a 50-Ω channel.

Keywords: UWB pulse, deliberate electromagnetic influences, interference protection, coupled lines, modal filter.

INTRODUCTION

Nowadays an important problem is protection of critical radio-electronic equipment from intentional electromagnetic influences [1–3]. Special attention is given to high-power electromagnetic nanosecond and subnanosecond pulses capable of penetrating into various radio-electronic systems and being attenuated only slightly by conventional protection devices [4–7]. Modal filters (MF) – passive structures capable of attenuating a UWB pulse by decomposing it into pulses with smaller amplitudes and different delays per unit length of signal modes propagating through the coupled line with non-uniform dielectric filling [8] – are promising protection devices. Essential MF advantages are their small mass, high reliability, and radiation resistance. Cable MF for power supply network [9, 10] and printing MF for Fast Ethernet [11] and protection against electrostatic discharges have already been investigated and manufactured [12]. In [13–16], results were presented of numerical simulation of the time domain response to a trapezoidal input pulse of the new structure of the printing MF – the asymmetric MF with facial feedback that differs by a simple design, high attenuation coefficient, and large difference between mode delays per unit length.

The present work is aimed at experimental investigation of UWB pulse propagation in the asymmetric MF of different cross sections with facial feedback and comparison of the experimental and simulated results with exact imitation of the real influence.

MODAL FILTER WITH FACIAL FEEDBACK

The main idea of modal filtration consists in the application of modal distortions (signal distortion due to different delays of the transverse wave modes in a multiwire transmission line) for protection. During propagation of the pulse excited in an active conductor of a line section with non-uniform dielectric filling consisting of *N* conductors

---

Tomsk State University of Control Systems and Radioelectronics, Tomsk, Russia, e-mail: alexandr.bbm@gmail.com; zabolotsky_am@mail.ru; talgat@tu.tusur.ru.
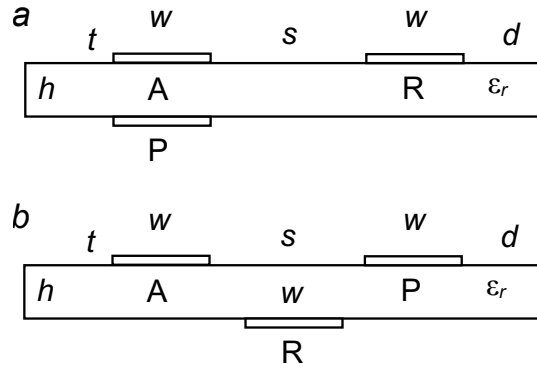
Fig. 1. MF cross section with facial (*a*) and end face (*b*) coupling.

(disregarding the reference conductor), it undergoes modal distortions up to decomposition into N pulses of smaller amplitudes because of the difference of the mode delays per unit length of the line [17]. For complete pulse decomposition, the condition

$$t_\Sigma < l \cdot \min|\tau_{i+1} - \tau_i|, \ i = 1, \ldots, N-1, \tag{1}$$

must be fulfilled, where t_Σ is the total pulse duration on the level 0, l is the section length, τ_i is the delay of the ith mode per unit length. In the particular case $N = 2$, condition (1) is reduced to the form

$$t_\Sigma < l \cdot |\tau_e - \tau_o|, \tag{2}$$

where τ_e and τ_o are delays of even and odd modes per unit length of the section of coupled lines.

Thus, if at the beginning of the section of the pair of coupled conductors between any of them and the common conductor the pulse is applied with duration smaller than the difference between the mode delays in this section, at the end of the section (between the same conductors) two pulses will arrive with amplitudes twice smaller than the amplitude of the pulse at the beginning of the section. It is established that an increase in electromagnetic coupling between the conductors of the coupled line leads to the decrease of the decomposition pulse amplitudes. For example, in [18] it was shown that a printed MF with facial (strong) feedback (Fig. 1*a*) can have the attenuation coefficient greater by a factor of 3.5 and the maximum duration of the decomposed pulse longer by 10 times compared to the structure with the end face (weak) coupling (Fig. 1*b*). As to the useful signal distortions, it is important to note that the MF is the low-pass filter. Therefore, for example, the useful signal with a spectrum in the MF passband will not undergo peak distortions.

Let us consider the MF cross section (invariable with length) with facial feedback (Fig. 1*a*): on the substrate of thickness h and dielectric permittivity ε_r three parallel conductors – active (A), reference (R), and passive (P) – are specially arranged. The width of the conductors is w, their thickness is t, the conductors are spaced at the distance s, and the distance from the edge of the structure to a conductor is d.

The circuit diagram of the MF is shown in Fig. 2. Here e denotes the EMF source, R_1 and R_3 denote resistances of the source and load, R_2 and R_4 denote the MF resistances, and U_1–U_3 designate nodes. The near and far ends of the active (A) and passive (P) conductors in the circuit are also designated.

DEVELOPMENT AND MANUFACTURE OF MODELS

The range of geometrical parameters for MF models was chosen proceeding from the requirements of miniaturization, economic expediency, and maximal transmitted current. From reasons of cheapness and accessibility, bilateral foiled fiberglass with parameters $h = 0.18$ mm and $t = 65$ μm was used. Genetic algorithms were employed for
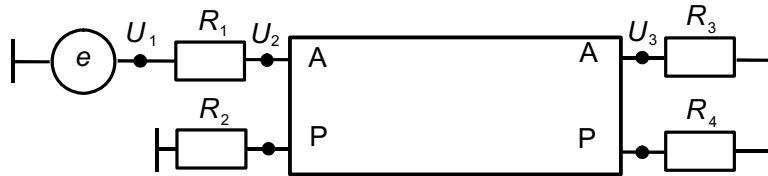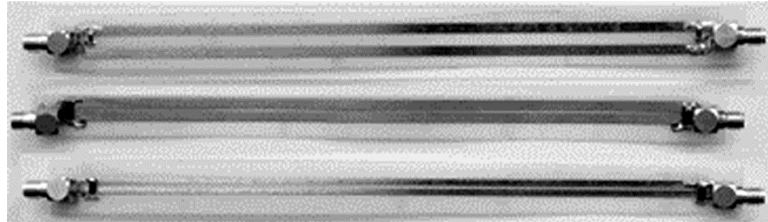
Fig. 2. Circuit diagram of the MF.
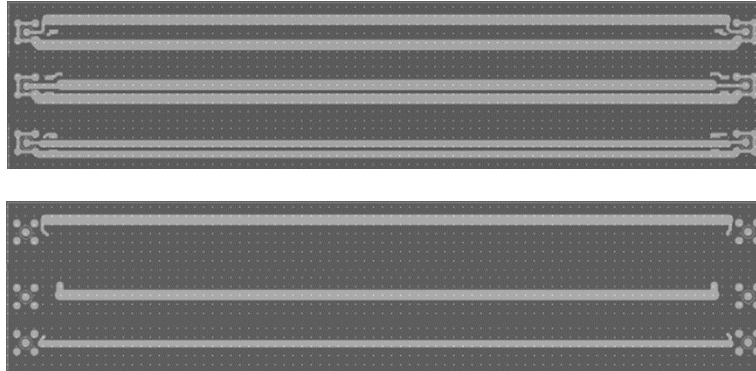

Fig. 3. Photograph of the MF models.

Fig. 4. Photomasks of two sides of the board with the MF.

computer simulation to determine the optimal parameter values of the TALGAT system [19] (by the criterion of maximal difference of mode delays per unit length): $s = 3$ mm and $w = d = 4$ mm for the MF in the channel with a 50-Ω wave resistance. The MF resistances $R_2 = R_4 = 50$ Ω were chosen for minimization of reflections. Additional models were manufactured to estimate roughly the sensitivity of the time domain response to the deviation from the optimal parameters of the conductors. The length of each model was 0.2 m. To connect with measuring devices, SMA-sockets were soldered to inputs and outputs of each model. For convenience, each model was given the serial number:

    1. MF model with $w = 3$ mm and $s = 4$ mm.

    2. MF model with $w = 3$ mm and $s = 1$ mm.

    3. MF model with $w = 2$ mm and $s = 1$ mm.

Photographs and photomasks of the models are shown in Figs. 3 and 4, respectively.

SIMULATION AND MEASUREMENT METHODS

To simulate the time domain response, a quasi-static analysis based on fast and exact mathematical models of the TALGAT system [20] was used. For this analysis, a simplifying assumption was made that there are no higher-order
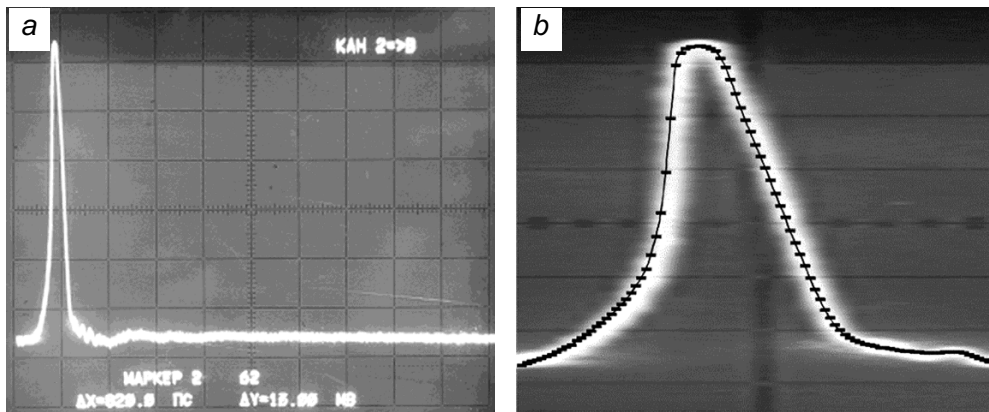
Fig. 5. Input influence (*a*), its image magnified along the abscissa, and its digital shape with markers in 10 ps (*b*).

waves in the lines, and only the *TEM* wave can propagate. This allowed the Maxwell equations to be reduced to cable equations whose solution is much easier, but is exact for most practical applications [21]. In the TALGAT system it is possible to analyze regular transmission lines with arbitrary cross section. The section of the transport line with the preset cross section, *N* signal conductors, and one reference conductor is described by the following matrices of the parameters per unit length: electromagnetic induction (**L**), electrostatic induction (**C**), resistance (**R**), and conductivity (**G**). The matrices **L** and **C** were calculated by the method of moments. Calculation of the matrix **C** for the examined case (the two-dimensional configuration with orthogonal boundaries) was described in detail in [22]. The matrix **L** is equal to the product of the magnetic permeability and dielectric permittivity of the free space multiplied by the inverse matrix **C** calculated for the case when the same geometry of conductors was placed in the free space [21]. The losses in conductors and dielectrics were determined by matrices **R** and **G**, respectively, taking into account their frequency dependence. The components of the matrix **R** were calculated taking into account the skin effect. All conductors had identical cross sections; therefore, the diagonal (r) and non-diagonal (r_m) components of the matrix **R** were related by the expression $r = 2r_m$, where $r_m = 1/(w\sigma t) + r_s/w$, σ is the specific conductivity of copper, w is the conductor width, $r_s = (\pi f \mu_0/\sigma)^{1/2}$, f is the frequency, and μ_0 is the absolute magnetic permeability. In the process of simulation it was assumed that the substrate, as at a frequency of 1 GHz, had $\varepsilon_r = 4.5$ and $\tan \delta = 0.025$ at all frequencies. For these values, the matrix **G** was calculated and recalculated for other frequencies. The matrix **G** was found by the method of moments, with the only difference that real dielectric constants were replaced by complex ones considering losses in dielectrics [23].

A periodic influence in the time domain was considered, and its fast Fourier transform was taken. For each frequency, the method of modified central matrix [24] was used to determine the voltage on a given node. The voltage in the time domain was obtained using the inverse Fourier transform.

The time domain response was measured with a C9-11 combined computing oscilloscope representing a combination of an UWB stroboscopic oscilloscope, a nano- and picosecond measuring pulse generator, and a built-in microcomputer. As an input influence, a 600-mV 820-ps (on a level of 0.1) pulse shown in Fig. 5*a* was applied (to a 50-Ω load). For simulaton, this signal was digitized and then used as an input influence for the TALGAT system (Fig. 5*b*).

RESULTS OF SIMULATION AND MEASUREMENT

Figure 6 shows the simulated and experimentally measured time domain responses of the models. Their quantitative characteristics are given in Table 1.

458

TABLE 1. Quantitative Comparison of the Results of Simulation (S) and Experiment (E); $\Delta = |(X_S - X_E)/(X_S + X_E)| \cdot 100\%$

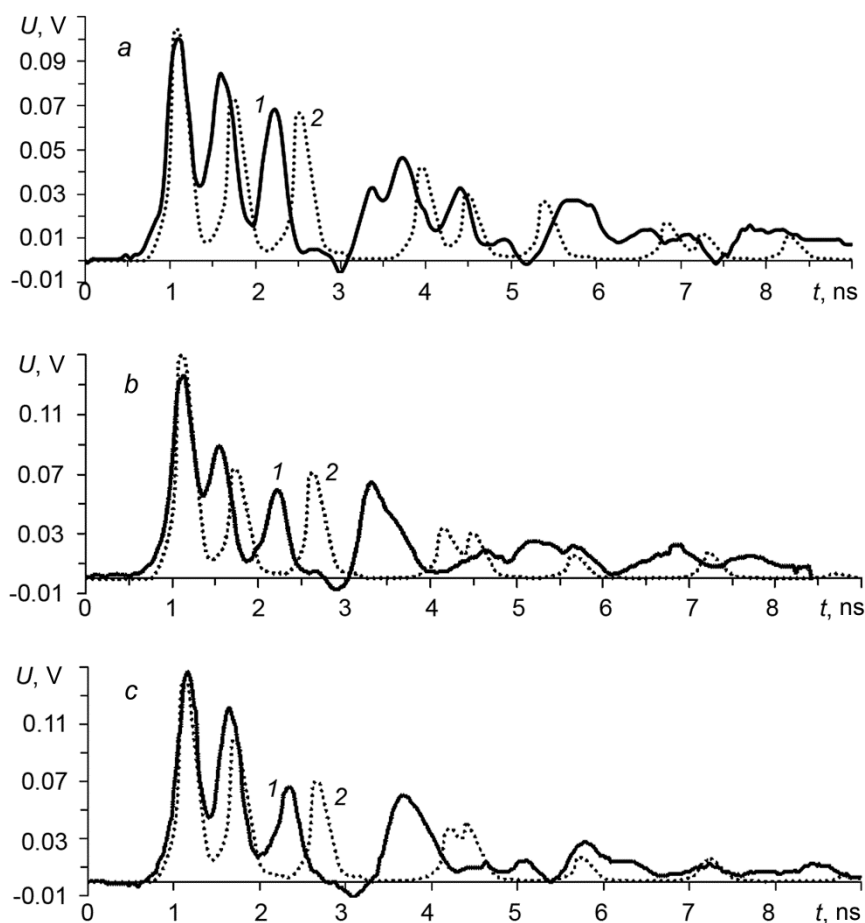| Model number	Peak value of the first pulse, mV			Peak value of the second pulse, mV			Difference between the time delays of the peak values, ns		
	S	E	Δ,%	S	E	Δ,%	S	E	Δ,%
1	100	113	6.1	65	90	16.1	0.72	0.6	9.1
2	143	145	0.7	72	95	13.8	0.67	0.6	5.5
3	145	153	2.7	97	120	10.6	0.69	0.6	7.0

Fig. 6. Results of measured (curve *1*) and simulated (curve *2*) time domain responses at the outputs of models 1–3 (*a–c*).

DISCUSSION OF RESULTS

According to the results obtained (Fig. 6 and Table 1), for all models we can note the following. The simulated pulse amplitudes at the output from the MF are smaller and the difference between the signal mode delays is greater than the corresponding measured values. The discrepancy between the delays per unit length is manifested in the obtained time domain responses as a delay between the simulated and measured time domain responses (Fig. 6). One of the reasons for such discrepancy can be the discrepancy between the value ε_r of the substrates used in simulation from

its true value. If the simulated ε_r value of the substrate is less than its true value, this explains a smaller difference between the pulse delays in the experiment. This, in turn, leads to imposition of the trailing edge of the first pulse on the leading edge of the second pulse; as a result, the amplitude of the second pulse increases. Therefore, the deviation of the experimental voltage from the simulated voltage of the second pulse is greater, than for the first pulse (as it follows from Table 1). The results of simulation and experiment differed also due to the fact that the actual MF sizes differed a little from the simulated ones. In addition, the influence (disregarded in simulation) is inevitable of the inhomogeneities of the SMA-sockers and their seats at the MF input and output as well as of the parasitic parameters of resistors, their transitive apertures, and seats. Finally, it is necessary to take into account that the limiting allowable error of time measurements for the C9-11 oscilloscope is 7.5 %. Thus, we can consider that the results of measurement and simulation are in agreement, and the reasons for their discrepancy have been established.

Let us consider the results for each model. Model 1 is the MF with optimal parameters and provides input pulse attenuation by approximately 5 times. From Fig. 6a it can be seen that the output signal represents a pulse train. The first pulse is the even mode, the second pulse is the odd mode, and the subsequent pulses are their reflections (from the line end and beginning) arriving with 3, 5, … delays in the line. Thus, the effect of the modal decomposition is confirmed, thereby allowing the output signal amplitude to be decreased. Model 2 has a shorter distance between the active and reference conductors compared to model 1, and model 3 has smaller widths of the conductors compared to model 2. As can be seen, the modal decomposition of pulses remains, but their attenuation decreases by about a factor of 1.5. This is explained by a decrease in the coupling between the active and passive conductors leading to an increase in the output amplitudes.

CONCLUSIONS

Thus, the physical process of electromagnetic wave propagation along the regular structure of coupled lines with resistive loads at the ends of this structure has been investigated. The non-uniform dielectric filling in the cross section of such structure leads to different delays of even and odd modes of the transverse electromagnetic wave per unit length. At certain parameters of lines, the electric pulse excited between the pair of conductors of the line leads to the interesting physical phenomenon of decomposition of this pulse into two pulses (even and odd modes). Moreover, an increase in electromagnetic coupling between the conductors of the structure can intensify this phenomenon: to increase the time interval between the pulses and to reduce their amplitudes. In addition, due to the increased difference between the impedances of even and odd modes, the other phenomenon: the multiple reflections of these pulses from the loads at the line ends with slow attenuation of reflected pulse amplitudes become more pronounced. As a matter of fact, the phenomenon of conversion of one pulse into a large number of pulses with smaller amplitudes on both ends of the structure is observed, and this phenomenon can be used for protection.

Of course, as can be seen from the plots, the allowance for the losses and the actual pulse shape will introduce corrections to the pattern of the described wave processes. In this work, the experimental investigation of the time domain response of the asymmetric MF with facial feedback to a 1-ns pulse with its subsequent simulation based on exact imitation of the pulse shape has been performed for the first time. This made significant contribution to the agreement between the results of experiment and simulation. However, the comparison has also revealed the necessity of a more exact allowance for the parameters of a real dielectric in the process of simulation. For maximal coupling and optimal parameters of the modal filter, the attenuation by 5 times was obtained in the 50-Ω channel. Meanwhile, this suggests that a more correct allowance for the losses in the conductors and dielectric and their use for the alignment of the pulse amplitudes for the even and odd modes will allow the attenuation to be increased significantly.

REFERENCES

1. GOST R 52863-2007, Protection of information. Protective automatically systems. Testing for stability to intentional power electromagnetic influence. General requirements, Standartinform, Moscow (2007).
2. N. Mora, F. Vega, G. Lugrin, *et al*., System and Assessment Notes. Note 41 (8 July, 2014).
3. GOST R 56103-2014, Information protection. Protected operational systems. Organization and content of operations on the protection against purposeful powerful electromagnetic impacts. General requirements, Standartinform, Moscow (2014).
4. R. M. Gizatullin, Z. M. Gizatullin, Noise Stability and Security of Information of Computer Facilities against Electromagnetic Impacts on Power Supply Network [in Russian], Publishing House of Kazan' State Technical University, Kazan' (2014).
5. T. R. Gazizov, A. M. Zabolotsky, A. O. Melkozerov, *et al*., in: Book of Abstracts EUROEM 2012, Toulouse (2012), p. 106.
6. K. Yu. Sakharov *et al*., Tekhnol. Elektromagn. Sovmest., No. 3 (18), 36–45 (2006).
7. T. Weber, R. Krzikalla, and L. Haseborg, IEEE Trans. Electromagn. Compatibility, **46**, No. 3, 297–304 (2004).
8. A. M. Zabolotsky and T. R. Gazizov, Modal Filters for Protection of Onboard Radio-Electronic Equipment of a Space Vehicle [in Russian], Publishing House of Tomsk University of Control Systems and Radioelectronics, Tomsk (2013).
9. T. R. Gazizov and A. M. Zabolotsky, IEEE Trans. Electromagn. Compatibility, **54**, No. 1, 229–231 (2012).
10. T. R. Gazizov, A. M. Zabolotsky, and I. E. Samotin, in: Proc. Int. Siberian Conf. on Control and Communications (SIBCON-2009), Tomsk (2009), pp. 264–269.
11. T. R. Gazizov, I. E. Samotin, A. M. Zabolotsky, and A. O. Melkozerov, in: Proc. 30th Int. Conf. on Lightning Protection, Cagliary (2010), pp. 1246-1–1246-3.
12. T. R. Gazizov, E. S. Dolganov, and A. M. Zabolotsky, Russ. Phys. J., **55**, No. 3, 282–286 (2012).
13. A. M. Zabolotskyand A. T. Gazizov, Int. J. Circuits Syst. and Signal Process., **9**, 68 (2015).
14. A. T. Gazizov and A. M. Zabolotsky, in: Proc. Int. Siberian Conf. on Control and Communications (SIBCON), Omsk (2015); DOI: 10.1109/SIBCON.2015.7147024.
15. A. T. Gazizov, A. M. Zabolotsky, and O. A. Gazizova, in: Proc. 16th Int. Conf. of Young Specialists on Micro/Nanotechnologies and Electron Devices EDM 2015, Erlagol (2015), pp. 120–123; DOI: 10.1109/EDM.2015.7184504.
16. A. T. Gazizov, in: Proc. ASIAEM 2015, Jeju Island (2015), pp. 232–234.
17. T. R. Gazizov and A. M. Zabolotsky, Tekhn. El. Magn. Sovmest., No. 4, 40 (2006).
18. A. T. Gazizov, in: Modern Problems of Radio Electronics [in Russian], Krasnoyarsk (2015), pp. 317-319 [Electronic resource]; Access mode: http://efir.sfu-kras.ru/wp-content/uploads/download/Сборник_СПР-2015.pdf.
19. S. P. Kuksenko, A. M. Zabolotsky, A. O. Melkozerov, and T. R. Gazizov T. R, Proc. TUSUR University, No. 2 (36), 45–50 (2015).
20. T. R. Gazizov, in: Proc. 2001 IEEE EMC Symp., Montreal (2001), pp. 151–155; DOI: 10.1109/ISEMC.2001.950576.
21. A. R. Djordjevic, T. K. Sarkar., and R. F. Harrington, Proc. IEEE, **75**, No. 6, 743–764 (1987).
22. T. R. Gazizov, Russ. Phys. J., **47**, No. 3, 326–328 (2004).
23. R. F. Harrington and C. Wei, IEEE Trans. Microwave Theor. Tech., **32**, 705–710 (1984).
24. J. R. Griffith and M. S. Nakhla, IEEE Trans. Microwave Theor. Tech., **38**, 1480 (1990).